

## Use of the Vis-SWIR to aid atmospheric correction of multispectral and hyperspectral thermal infrared (TIR) imagery: The TIR model

John Gruninger<sup>\*a</sup>, Marsha Fox<sup>a</sup>, Jamine Lee<sup>a</sup>, Anthony J. Ratkowski<sup>b</sup> and Michael L. Hoke<sup>b</sup>

<sup>a</sup>Spectral Sciences, Inc., <sup>b</sup>Air Force Research Laboratory, Space Vehicles Directorate

### ABSTRACT

The atmospheric correction of thermal infrared (TIR) imagery involves the combined tasks of separation of atmospheric transmittance, downwelling flux and upwelling radiance from the surface material spectral emissivity and temperature. The problem is ill posed and is thus hampered by spectral ambiguity among several possible feasible combinations of atmospheric temperature, constituent profiles, and surface material emissivities and temperatures. For many materials, their reflectance spectra in the Vis-SWIR provide a means of identification or at least classification into generic material types, vegetation, soil, etc. If Vis-SWIR data can be registered to TIR data or collected simultaneously as in sensors like the MASTER sensor, then the additional information on material type can be utilized to help lower the ambiguities in the TIR data. If the Vis-SWIR and TIR are collected simultaneously the water column amounts obtained from the atmospheric correction of the Vis-SWIR can also be utilized in reducing the ambiguity in the atmospheric quantities. The TIR atmospheric correction involves expansions in atmospheric and material emissivity basis sets. The method can be applied to hyperspectral and ultraspectral data, however it is particularly useful for multispectral TIR, where spectral smoothness techniques cannot be readily applied. The algorithm is described, and the approach applied to a MASTER sensor data set.

**Keywords:** Hyperspectral, Multispectral, Atmospheric Correction, Data fusion

### 1. INTRODUCTION

Space-based Thermal IR (TIR) imagery is a powerful remote sensing method that can operate in nighttime, fog and haze conditions. We include in the thermal infrared all emission dominated radiance in the MWIR and LWIR between 4-15  $\mu\text{m}$ . Several approaches for enhancing the information content of TIR imagery have been studied in recent years, including increasing the spectral resolution to the hyperspectral or ultraspectral level. High spectral resolution is valuable for retrieving atmospheric properties and for separating surface temperature and emissivity. Currently, ambiguities in separating temperature, emissivity and atmospheric effects complicate the interpretation of the imagery using multiple wavelength bands. High spectral resolution TIR requires a larger spatial footprint for an equivalent signal-to-noise than multispectral TIR. The large footprints make the detection of small objects more difficult. The approach of fusing multispectral TIR imagery with short-wave data helps overcome these problems and has several other important practical advantages. Vis-SWIR data can be collected ahead of time, even several days in advance, and from a different platform than the TIR sensor's. The Vis-SWIR data must be collected during the day, and such sensors generally have very good signal-to-noise and spatial resolution. TIR provides for both day and night observations.

The material reflectance spectra in the Vis-SWIR provide a means of identification or at least classification into generic material types, vegetation, soil, etc. If Vis-SWIR data can be registered to TIR data or collected simultaneously, as with sensors such as the MASTER sensor, then the additional information on material type can be utilized to help lower the ambiguities in the TIR data. In this effort we apply FLAASH<sup>1</sup> to Vis-SWIR to obtain reflectance maps. These are used to identify materials by matching scene reflectances with library reflectances.

To ensure that the scene reflectances correspond more closely to single materials, we use SMACC,<sup>2</sup> an end-member code, to determine the unique pixel spectra in the scene. Identification of a material type is not always sufficient to

---

<sup>\*</sup> john@spectral.com; phone: 781 273-4770; fax: 781 270-1161; <http://www.spectral.com>; Spectral Sciences, Inc., 99 South Bedford Street, Burlington MA, USA 01803-5169.

Report Documentation Page				Form Approved OMB No. 0704-0188	
Public reporting burden for the collection of information is estimated to average 1 hour per response, including the time for reviewing instructions, searching existing data sources, gathering and maintaining the data needed, and completing and reviewing the collection of information. Send comments regarding this burden estimate or any other aspect of this collection of information, including suggestions for reducing this burden, to Washington Headquarters Services, Directorate for Information Operations and Reports, 1215 Jefferson Davis Highway, Suite 1204, Arlington VA 22202-4302. Respondents should be aware that notwithstanding any other provision of law, no person shall be subject to a penalty for failing to comply with a collection of information if it does not display a currently valid OMB control number.					
1. REPORT DATE <b>2006</b>		2. REPORT TYPE		3. DATES COVERED <b>00-00-2006 to 00-00-2006</b>	
4. TITLE AND SUBTITLE <b>Use of the Vis-SWIR to aid atmospheric correction of multispectral and hyperspectral thermal infrared (TIR) imagery: The TIR model</b>				5a. CONTRACT NUMBER	
				5b. GRANT NUMBER	
				5c. PROGRAM ELEMENT NUMBER	
6. AUTHOR(S)				5d. PROJECT NUMBER	
				5e. TASK NUMBER	
				5f. WORK UNIT NUMBER	
7. PERFORMING ORGANIZATION NAME(S) AND ADDRESS(ES) <b>Spectral Sciences Inc,4 Fourth Avenue,Burlington,MA,01803-3304</b>				8. PERFORMING ORGANIZATION REPORT NUMBER	
9. SPONSORING/MONITORING AGENCY NAME(S) AND ADDRESS(ES)				10. SPONSOR/MONITOR'S ACRONYM(S)	
				11. SPONSOR/MONITOR'S REPORT NUMBER(S)	
12. DISTRIBUTION/AVAILABILITY STATEMENT <b>Approved for public release; distribution unlimited</b>					
13. SUPPLEMENTARY NOTES					
14. ABSTRACT					
15. SUBJECT TERMS					
16. SECURITY CLASSIFICATION OF:			17. LIMITATION OF ABSTRACT	18. NUMBER OF PAGES <b>13</b>	19a. NAME OF RESPONSIBLE PERSON
a. REPORT <b>unclassified</b>	b. ABSTRACT <b>unclassified</b>	c. THIS PAGE <b>unclassified</b>			

determine the reflective properties, particularly of natural materials. Various states of health and leaf cover lead to a wide variety of vegetation reflectance spectra. Vegetation spectra in the Vis-SWIR are used to remotely determine vegetation conditions.<sup>3</sup> These variations extend into the TIR. The use of basis sets which include these variations have been applied to successfully unmix pixel spectra.<sup>4,5,6</sup> If the Vis-SWIR and TIR are collected simultaneously, the water column amounts obtained from the atmospheric correction of the Vis-SWIR can also be utilized to reduce the ambiguity of the atmospheric quantities in TIR imagery.

In this paper we address multispectral TIR atmospheric correction, a critical step in the fusion process. Several efforts have been made to perform atmospheric correction on hyperspectral TIR data. These include the in-scene atmospheric correction method, ISAC,<sup>7</sup> which finds scaled estimates of atmospheric transmittance and path radiance. It must be applied to blackbody pixels, water or high emissivity vegetation areas. The method requires a statistical sampling of high emissivity pixels over a range of ground temperatures, making it difficult to apply to all scenes. For low emissivity materials in the corrected scene, a source term is derived that includes contributions from reflected downwelling atmospheric radiance.

Several methods use forward modeling including a look-up table (LUT) approach based on a grid of MODTRAN calculations<sup>8</sup> and spectral smoothness<sup>9</sup>. The approach provides a complete separation of the scene into pixel emissivities, temperatures and atmospheric profiles. Material emissivities are spectrally smooth compared to gas phase atmospheric absorption and emission features. Broad channels in multispectral sensors limit the utility of the smoothness criterion for such sensors. Other forward models use grids of calculations to form bases utilizing component analysis. Hernandez-Baquero and Schott<sup>10</sup> have developed an atmospheric correction model based on canonical correlation analysis, CCA. This method correlates a basis of atmospheric transmittance, path radiance and downwelling radiance to the scene radiances to select an atmosphere, and is followed by a temperature emissivity separation step. The method shows promise, however the correlation coefficients coupling the three atmospheric quantities to total radiance are different and the atmosphere selected does not necessarily correspond to a single profile. Villeneuve and Stocker<sup>11</sup> have developed OPRA, an oblique projection technique to perform atmospheric correction. Using a grid of atmospheric transmittances and path radiances computed from MODTRAN, OPRA uses two oblique subspace projections to estimate the atmospheric path radiance and transmittance separately. Independent projections can lead to the transmittance and path radiance being modeled in different regions of the subspaces and, hence, the predicted atmospheric quantities need not correspond to a single atmospheric profile. It is currently implemented for blackbody or highly emissive materials. Healey and Slater<sup>12</sup> use library reflectance spectra and generate a grid of radiances for a material for a wide range of atmospheric conditions and illumination. Basis sets formed from these radiances span subspaces for atmosphere and environment independent material detection.

The basis of our approach is a forward model that involves creation of a set of radiances that span the space of the scene pixel radiances and use a physically constrained least squares approach to simultaneously estimate the atmospheric quantities and the ground material emissivity and temperature. Atmospheric downwelling effects are included. The estimated atmospheric quantities are traceable to a single atmospheric profile. The methodology is described in Section 2. Initial applications of the method are described in Section 3.

## 2. TIR ATMOSPHERIC CORRECTION ALGORITHM

The radiance model is briefly described and then the atmospheric correction strategy is developed. Throughout this text we suppress the spectral index for simplicity. However, each of the radiative transport terms is dependent on the spectral wavelength interval. The quantities that we generate are the mean emissivity and the mean emission of a pixel. We consider the most general case of a mixture of materials in a pixel at a variety of temperatures. In this case the mean emission is not due to a single emissivity blackbody product, but rather from a sum of such products.

The model used for the radiance at the sensor,  $L$ , of a mixed pixel is

$$L = \overline{Em\pi} + (1 - \overline{e})D + U \quad (1)$$

and the radiance at the source,  $S$ , is given by

$$S = (L - U) / \tau \quad (2)$$

where  $D$  is the downwelling radiance that is transported to the observer,  $U$  is the upwelling or path radiance,  $\tau$  is the direct ground to observer transmittance,  $\bar{e}$  is the mean pixel emissivity and  $\overline{Em}$  is the mean pixel source emission. The mean emissivity of a pixel containing  $r$  materials is given by

$$\bar{e} = \sum_p^r \varepsilon_p a_p \quad (3)$$

where  $\varepsilon_p$  is the spectral emissivity of material  $p$  and  $a_p$  is the abundance of material  $p$  in the pixel. The abundances sum to unity,  $\sum_p^r a_p = 1$ . It follows that the mean source emission is given by

$$\overline{Em} = \sum_p^r \varepsilon_p a_p \sum_l^s f_{p,l} B(T_l) \quad (4)$$

where  $f_{p,l}$  is the fraction of material  $p$  that is at temperature  $T_l$ . The temperature distributions of each material must also sum to unity,  $\sum_l^s f_{p,l} = 1$ .  $B(T)$  is the Planck blackbody function. There are a total of  $r$  materials at  $s$  temperatures in the FOV.

This model includes all of the atmospheric interactions of importance for the TIR. The downwelling radiance is composed of indirect scattered radiance and atmospheric thermal emission. The model currently ignores reflected emissions from other ground sources, a component that will be added to the model in the future. The total hemispherical reflectance,  $\bar{\rho} = 1 - \bar{e}$ , is used in place of the full BRDF (Bi-directional Reflectance Distribution Function). Bi-directional reflectance effects are small in the TIR spectral region where emission dominates. The effects of directional emissivity can be included into the pixel source emission term. Directional effects will be more important when processing data sets collected at off nadir angles.

The basic problem of atmospheric correction in the TIR is the uncoupling of the atmospheric and material contributions, that is, atmosphere profile, emissivity and temperature separation. Strong coupling among the quantities, together with the sensitivity of the ground temperature predictions and lower altitude atmospheric temperature predictions to small variations in emissivity, make extraction of the of the atmospheric and the ground quantities very difficult. Initial guesses to any of these quantities strongly influence the predicted results for the other two quantities. We developed a solution via a triple expansion, with simultaneous extraction of atmospheric quantities, emissivities and temperatures.

A radiance basis is constructed by combining atmospheric and material emissivity and temperature basis sets. The atmospheric basis is obtained by running SMACC on a look-up table formed from a set of MODTRAN calculations that tabulate the transmittance, upwelling and downwelling radiance, that we refer to as the TUD, for a grid of atmospheric representations  $\{t_k, U_k, D_k\}$ . The index  $k$  designates position within the spanned atmospheric parameter space. A basis set of material emissivities,  $\{e_m\}$  can be selected from library or previously processed data. The emissivity basis should be selected to span the anticipated ground emissivities  $\{\varepsilon_p\}$ . Finally, a set of temperatures,  $\{T_n\}$  can be selected that span the anticipated ground temperatures, and a basis of blackbody emissions is formed using the Planck radiance expression. A radiance basis is constructed from the three sets by combining all possible combinations of atmospheric profile, emissivity and temperature. The set of radiances,  $\{\Lambda_{k,m,n}\}$ , is given by

$$\Lambda_{k,m,n} = e_m B(T_n) t_k + (1 - e_m) D_k + U_k \quad (5)$$

Formally, the pixel radiance can be estimated by calculating

$$\min || L - \sum_{k,m,n} \Lambda_{k,m,n} C_{k,m,n} || \quad (6)$$

with respect to the coefficients  $C_{k,m,n}$ , subject to physical constraints, i.e. by solving a constrained least squares problem. The radiance basis is constructed from the TUD basis, the emissivity basis and a grid of temperatures using Equation 5 rather than performing MODTRAN runs for each profile, emissivity and temperature. This leads to significant reductions in processing time, since each MODTRAN calculation needs only to be performed once per profile, and not repeated for each emissivity and temperature combination.

Once the expansion coefficients have been found, the estimates of the atmospheric transmittance, downwelling and upwelling path radiance are given by

$$\tau = \sum_{k,m,n} t_k C_{k,m,n}, D = \sum_{k,m,n} D_k C_{k,m,n} \text{ and } U = \sum_{k,m,n} U_k C_{k,m,n}, \text{ respectively.} \quad (7)$$

The expansion coefficients are the same for all three quantities, allowing the three atmospheric quantities to be derived from a single profile. If the coefficients are constrained to be positive, the resulting combination of the basis provides an interpolation of the basis atmospheres as the estimate to the unknown atmospheric TUD. Other estimated quantities include the emissivity, source emission, apparent blackbody emission and apparent temperature.

The emissivity of the pixel can be obtained from the reflected downwelling contribution,

$$\bar{\varepsilon} = \frac{\sum_{k,m,n} e_m D_k C_{k,m,n}}{\sum_{k,m,n} D_k C_{k,m,n}}. \quad (8)$$

It is a weighted average of the basis of emissivities used in the calculations. The ground material emission is determined from

$$\overline{Em} = \frac{\sum_{k,m,n} e_m B(T_n) t_k C_{k,m,n}}{\sum_{k,m,n} t_k C_{k,m,n}}. \quad (9)$$

If it is further assumed that either a single material is present within the footprint of the pixel or that all materials within the footprint are at the same temperature, the emission can be factored into an apparent Planck blackbody function,

$$B_{app} = \frac{\sum_{k,m,n} e_m B(T_n) t_k C_{k,m,n}}{\sum_{k,m,n} e_m t_k C_{k,m,n}}. \quad (10)$$

Also, an additional expression for the ground emissivity can be obtained as

$$\varepsilon = \frac{\sum_{k,m,n} e_m B(T_n) t_k C_{k,m,n}}{\sum_{k,m,n} B(T_n) t_k C_{k,m,n}} . \quad (11)$$

The two emissivity estimates, Equations 8 and 11, should agree closely for pixel ground materials at the same temperature. The apparent temperature is obtained as a function of the brightness temperature of the apparent blackbody emission.

Refined estimates to the atmospheric and ground quantities can be made based on a finer grid of basis functions centered around the current output estimates, or on additional criteria such as emissivity spectral smoothness, or smoothing the apparent blackbody estimate by selecting a single temperature from the spectrally dependent brightness temperatures retrieved from the apparent blackbody function, Equation 10.

Implementation of the simultaneous approach leads to a large basis set. For example, if there are 25 atmospheric basis functions, 4 emissivity basis functions and 2 temperatures, then the total number of radiance basis functions is  $25 \times 4 \times 2 = 200$ . The basis will generally be redundant and, as written, the formal solution is underdetermined. The rank or the number of linearly independent basis spectra will be less than the number of radiance basis spectra. This means that there are many possible solution vectors. The most that can be simultaneously taken as independent equals the number of spectral bands, but the actual number may be far fewer since the spectra are highly correlated for these wavelengths.

There are several approaches that can be taken to solve the underdetermined constrained equations. We seek an approach that will allow us to obtain estimates of the atmospheric and material properties. Here we consider the combined use of constraints and a singular value decomposition (SVD) basis. This leads to a new set of equations that is not underdetermined. We form a matrix,  $\Lambda$  of radiances whose columns are the  $\{\Lambda_{k,m,n}\}$ . Singular value decomposition can be applied to the  $\Lambda$  matrix. The expansion can be performed using the significant singular vectors, those with large singular values, rather than the  $\Lambda$  basis directly. The singular vectors with non-zero singular value form a linearly independent set. The SVD is given as

$$\Lambda = W_S V^T . \quad (12)$$

The columns of the matrix  $W$  are the left singular vectors, the basis spectra that will be used in the expansion. The matrix  $S$  is square and diagonal and contains the non-zero singular values on its diagonal, and the matrix  $V$  contains as its columns the right singular vectors. The new problem is to find the vector  $x$  whose elements satisfy

$$\min || L - \sum_i w_i x_i || \quad (13)$$

subject to the constraints on the elements of  $x$  that contributions of the redundant  $\Lambda$  basis remain positive. The constraints placed on  $x$  can be expressed in terms of the back-transformation

$$V_S^{-1} x = C . \quad (14)$$

The constraint relations are

$$V_S^{-1} x \geq 0 . \quad (15)$$

To solve the underdetermined problem posed by Equation 6, we solve the fully determined Equation 13, then back-transform via Equation 14 to obtain the set of coefficients,  $C_{k,m,n}$ .

The individual coefficients,  $C_{k,m,n}$ , are not well estimable due to the high correlation among the columns; however, the linear combinations of the columns that lie in the subspace of the dominant singular vectors are estimable.<sup>13</sup>

The set of coefficients,  $C_{k,m,n}$ , derived here are unique in that they are all positive or zero and they are the components of the solution vector of shortest length.<sup>14</sup> The SVD approach with constraints leads to a physically possible solution. We use the back-transformed coefficients to estimate the unknown atmospheric and material quantities as outlined above.

An alternative approach to determining a reduced basis is to use an end-member procedure to find a linearly independent set of vectors in the radiance basis. In the work described here we used a hybrid approach, using SMACC to find a basis to represent an atmospheric look-up table, then performing a SVD on the radiance basis constructed with the reduced atmospheric basis, emissivity basis and a grid of temperatures.

### 3. APPLICATION OF THE TIR ATMOSPHERIC CORRECTION METHOD

The initial testing of the algorithm included synthetic radiances constructed from a loam emissivity at a specified ground temperature and a selected atmosphere from a LUT. The selected atmosphere was not among those selected as a basis to represent the LUT, rather it was the atmosphere that was least well represented by the selected basis. The synthetic unknown is used to evaluate the ability of the algorithm to extract atmospheric and material quantities for situations in which the basis of atmospheres, emissivities and temperatures span or approximately span the simulated radiance and for cases where one of the quantities is not well represented. Given the constraints, a radiance spectrum will be in the span of our basis if the atmospheric quantities are represented by a positive linear combination of TUD basis members, the emissivity is represented by a weighted average of the emissivity basis and the ground temperature lies within the range of selected temperatures.

An atmospheric transmittance, upwelling and downwelling radiance (TUD) look-up table was generated for the MASTER sensor<sup>15</sup> mid-wave and long-wave IR channels. The atmospheric profile characteristics, water vapor column amounts and profile temperatures, and sensor altitude were selected so that the TUD would be appropriate for processing a MASTER California agriculture data cube that had been processed in the Vis-SWIR with FLAASH.

The atmospheric temperature profile model requires four temperatures and altitudes to specify it, see Figure 1. The top two altitudes and temperatures are above the sensor altitude of 3.18 kilometers. The altitudes for  $T_1$ ,  $T_2$ ,  $T_3$  and  $T_4$  were selected as 0km, 2km, 7km and 13km, respectively. An altitude range can be specified for which the temperature profile remains constant at  $T_3$ , but in this case it was specified at a point. All profiles in the TUD had the same upper atmospheric profile with temperature values  $T_3=255K$  and  $T_4=215K$ . An equally spaced grid of atmospheric temperatures at the ground,  $T_1$ , ranging from 280K to 310K, was selected. The equally spaced second temperature grid  $T_2$  at 2 kilometers was selected to range from 268K to 288K. The grid of water vapor column amounts for the TUD ranged from 70% to 100% of a standard humidity profile that is similar to the mid-latitude summer profile contained in MODTRAN. A basis to represent the TUD was obtained by using SMACC to determine the endmembers of the TUD. The endmember basis is determined sequentially with an improved representation of the TUD at each step. At each step the atmosphere which is least well approximated by the basis is added to the basis. A total of twenty five endmembers were found to adequately represent the remaining TUD members.

The synthetic unknown radiance spectrum was constructed from an atmosphere in the TUD. The selected atmosphere was not part of the basis. It was selected as the one which was least well approximated by the basis. This selection should test the ability of the basis to model any atmosphere within the convex span of the LUT's atmospheres. The lower atmosphere temperature,  $T_1$ , of this atmosphere was the hottest in the LUT,  $T_1=310K$ . The value of  $T_2=276K$  was a mid-value in the LUT. The water vapor content was the lowest possible in the LUT table, a value of 70% of the standard profile. This particular atmosphere was excluded from consideration for the basis. A loam spectrum from the ASTER library<sup>16</sup> was selected to represent the ground material. Its library number is 87P4453c and it is described as a "very dark grayish-brown loam". This spectrum was excluded from the emissivity basis sets, although five other loam spectra were used to form a loam emissivity basis. The ground temperature for the synthetic unknown radiance spectrum was set at 300K, a full 10K below the lower atmospheric temperature,  $T_1$ .

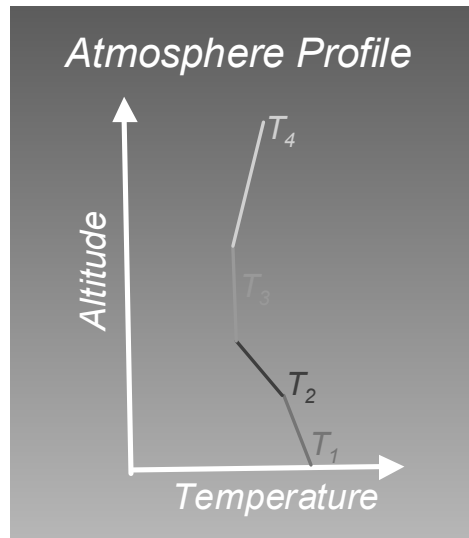


**Figure 1.** Definition of temperature profile for atmospheric TUD calculations.

The radiance basis for the calculations was constructed from the endmember basis of the TUD together with various combinations of emissivity bases and ground temperature grids. As a preliminary test, we used the same material emissivity in the basis as in the unknown. This let us determine the adequacy of the atmospheric endmembers to describe the unknown atmosphere and the feasibility of using a grid of ground temperatures to estimate the true ground temperature. We also performed calculations using a spanning basis of other loam emissivities that did not contain the actual ground emissivity spectrum and a non-spanning basis that consisted of vegetation spectra. The results showed the sensitivity of the atmosphere and temperature determination to emissivity estimates. The results for the non-spanning emissivity basis lead to unphysical atmospheric quantities and poor ground temperature estimates. The results for incorrect guesses of ground temperature lead to poor estimates of emissivity and poor or unphysical estimates of the atmospheric quantities. The results for a grid of two temperatures, which bracketed the actual ground temperature, were as good as guessing the temperature exactly, and the ground temperature could be extracted from the brightness temperature of the estimated blackbody function.

The results for several of the initial calculations are summarized in Figure 2. Calculations labeled “truth” in Figure 2 correspond to the inputs to the test radiance. The atmospheric basis was used for all other calculations. Calculations labeled “Full Model” use the emissivity basis that includes other loam spectra and a pair of ground temperatures, 298K and 302K which bracket the test ground temperature of 300K. Calculations labeled “Model  $\epsilon$  known” use the same emissivity spectrum as the test calculations and the pair of ground temperatures, 298K and 302K which bracket the test ground temperature of 300K. Calculations labeled “Model T=298K” and “Model T=302K” use the basis of ground emissivities and single ground temperatures which are too low and too high, respectively. Calculations labeled “Model  $\epsilon$  = vegetation” used an emissivity spectrum of vegetation and the pair of ground temperatures of 298K and 302K. The closeness of the “Model  $\epsilon$  known” results to the “Truth” indicate that the atmospheric basis does span the atmospheres in the LUT and that adequate ground temperature estimates can be made by selecting a sufficient grid of ground temperatures as model input. The agreement of the “Full Model” with the “Truth” in Figure 2 gives an indication of the agreement that can be expected for favorable conditions of a spanning atmospheric basis, a spanning ground emissivity basis and a pair of bracketing temperatures. The remaining calculations illustrate the effects of selecting a model ground temperature too low or too high, or of selecting the ground emissivity of the wrong material type. If the model temperature is selected too low, 298K, an incorrect atmosphere with a higher low atmospheric temperature  $T_1$  results, and the predicted emissivity is too high and has an incorrect shape. If the model temperature is too high, 302K, an incorrect atmosphere with a lower low atmospheric temperature,  $T_1$  results and the predicted emissivity is too low and has the wrong shape. If an incorrect emissivity spectrum is selected, vegetation in place of loam, the overall shapes of the predicted atmospheric quantities are in disagreement with the true quantities and the ground temperature is estimated as 299.5K.

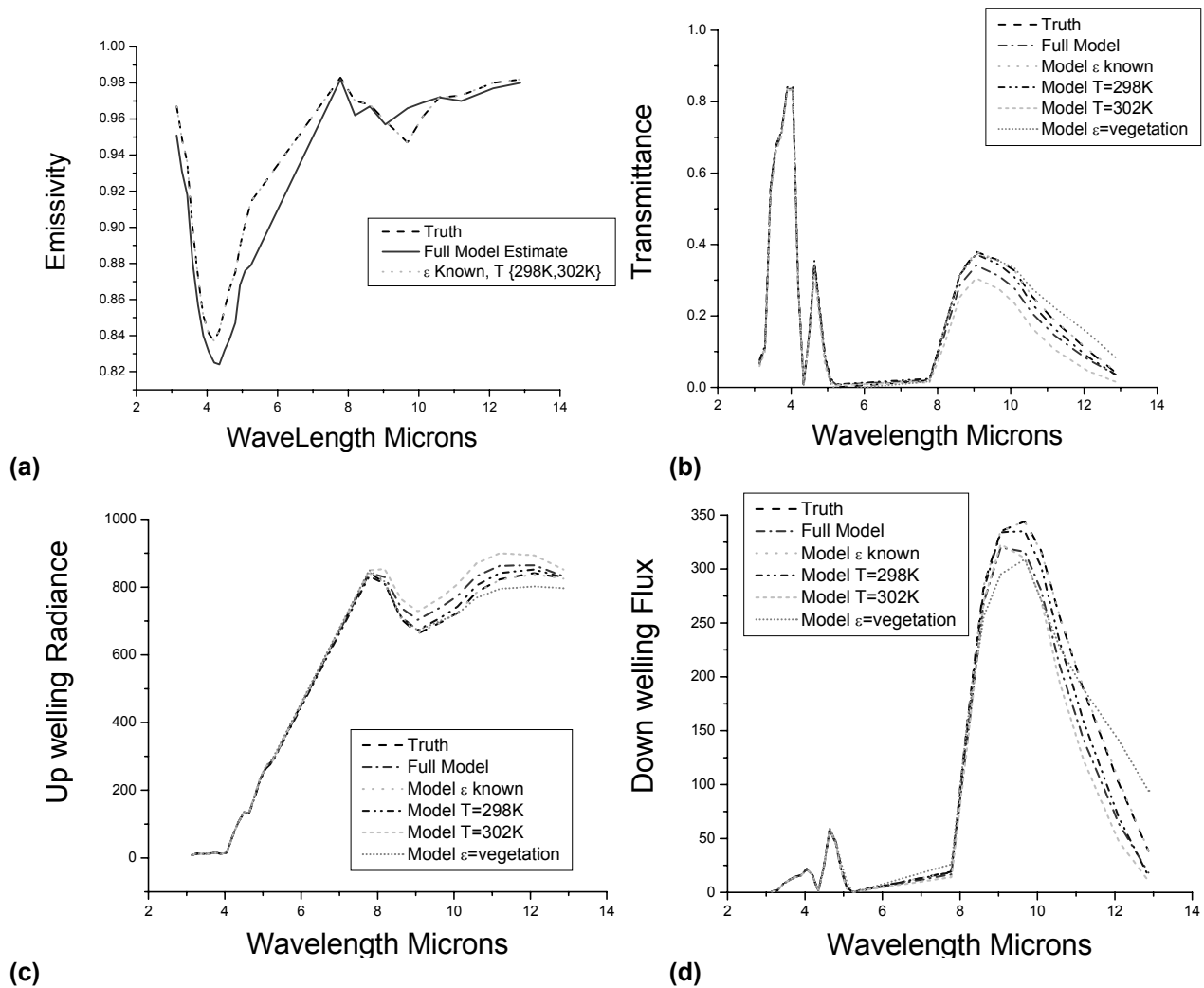


**Figure 2.** Results of calculations estimating the emissivity (a), transmittance (b), upwelling radiance (c) and downwelling flux (d) compared with the synthetic unknown radiance inputs (Truth).

### Application to the MASTER Scene

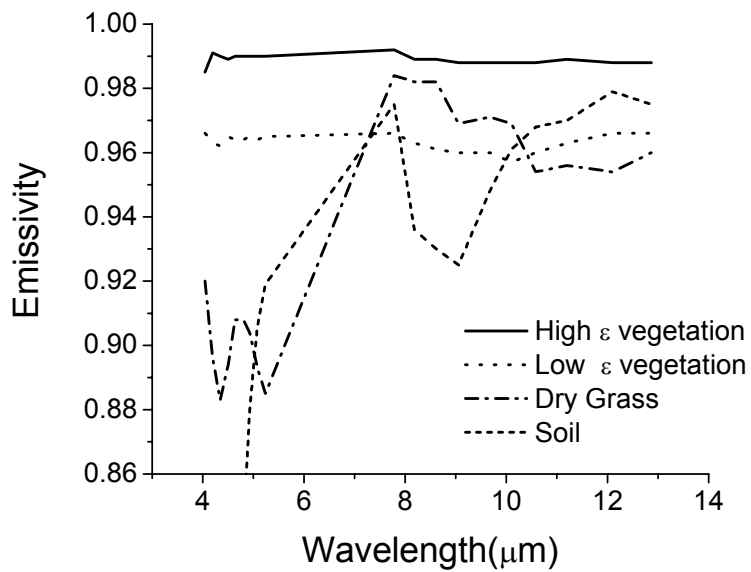
The first application we made of the multispectral TIR atmospheric correction approach to real data was to a MASTER sensor California agricultural scene illustrated in Figure 3. FLAASH was used to determine reflectances in the Vis-SWIR as well as the humidity and visibility. SMACC was used to determine endmember reflectances in the VIS-SWIR and the reflectance endmembers were matched against library spectra to identify material type. The endmember material abundances were used to determine groups of spectra of the same type. The groups with large numbers of pixel spectra were chosen for atmospheric correction. Nine endmember groups were selected. These groups were primarily varieties of vegetation with some soil with one group being primarily soil.

The emissivity basis used for the calculations included four spectra: two green vegetation spectra, one of high emissivity and one of low emissivity, a dry grass spectrum and a soil spectrum. The vegetation emissivity spectra were taken from those made available by Wan<sup>17</sup>. The spectra illustrate the variability of reflectance properties of vegetation in the TIR spectral region. The soil spectrum is the average spectrum of 25 ASTER library soil emissivity spectra. The spectra are illustrated in Figure 4.



**Figure 3.** MASTER California agricultural scene.

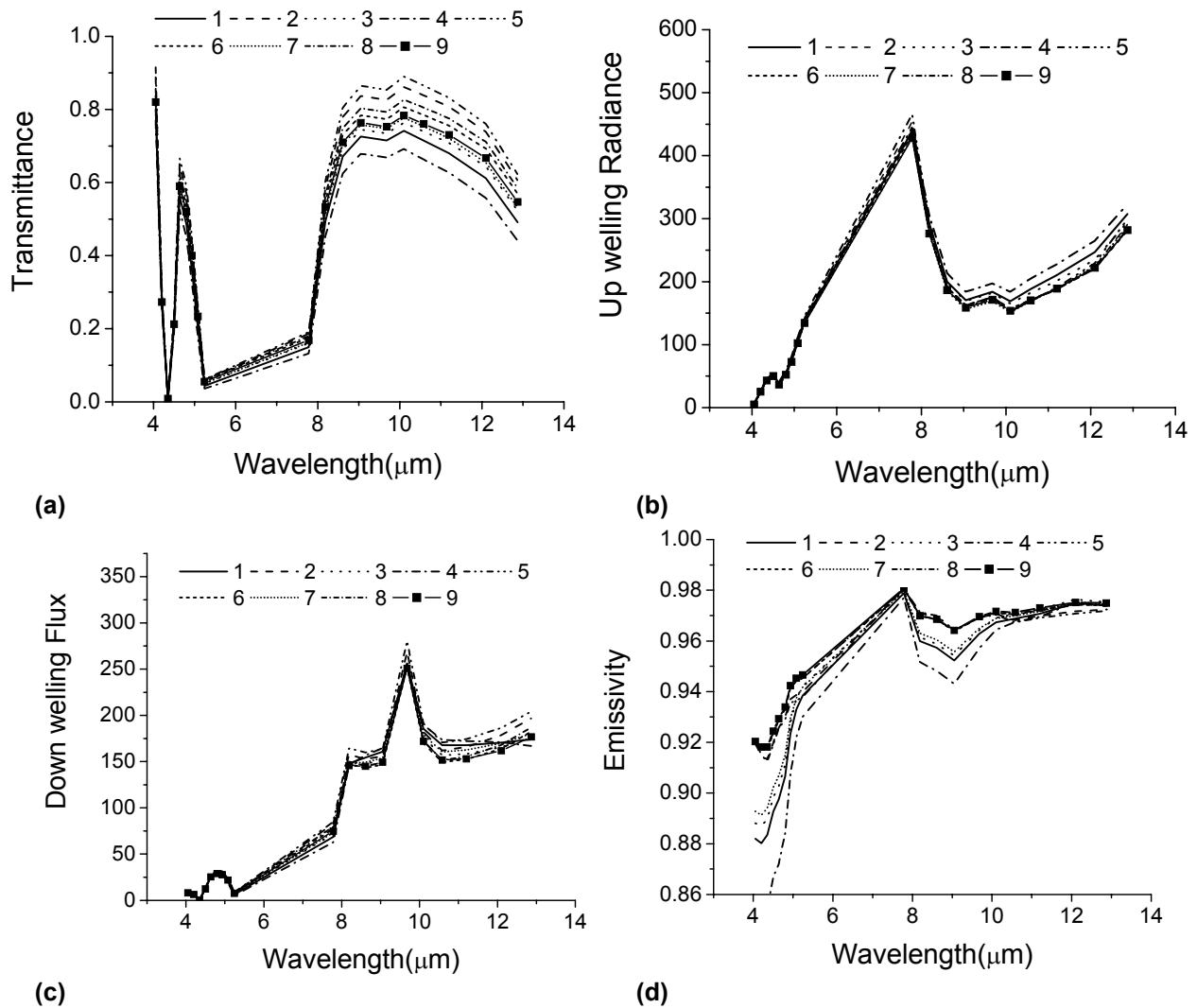
An initial range of bracketing ground temperatures was chosen between 290K and 310K, then narrowed to 296K and 304K. The ability to successfully use the linear approximation to unmix TIR data has been recently illustrated.<sup>18</sup>



**Figure 4.** Emissivity Basis for calculations include a high emissivity chlorophyll containing vegetation spectrum, a low emissivity chlorophyll containing vegetation spectrum, a dry grass spectrum and a soil spectrum.

Two atmospheric basis sets were utilized, the one used in the application to the synthetic spectrum, and a second smaller basis derived from an atmospheric LUT in which the humidity was restricted to 3085.5 atm-cm, the value retrieved from the Vis-SWIR spectral region using FLAASH. In this smaller LUT the upper atmospheric temperatures were held fixed and the lower temperatures were varied from 290K to 310K for  $T_1$  and 280K to 300K for  $T_2$ . Differences among the resulting atmospheric corrections obtained from the two atmospheric basis sets illustrate the advantages of fully utilizing results of atmospheric correction of Vis-SWIR data to aid in the TIR atmospheric correction.

Results for the two sets of calculations applied to the nine endmember groups are reported in Figures 5 and 6 for the atmospheric basis with variation in atmospheric humidity and for the atmospheric basis with humidity restricted, respectively. Differences between the two sets of calculations include a much narrower spread in ground temperatures but a broader spread in lower atmospheric temperature for the variable humidity atmospheric basis. Both humidity and lower atmospheric temperature variations contribute to the variability among predicted atmospheric transmittance, and upwelling and downwelling radiance. The ground temperature and the downwelling radiance estimations are the most sensitive to the small differences in extracted emissivity. These are the quantities that are the most different for the two sets of calculations. For high emissivity materials the downwelling contribution to the radiance is small, and moderate to large variations in the downwelling radiances lead to very small changes in total radiance. The use of the auxiliary information obtained from FLAASH about the atmosphere leads to a greater relative consistency for the predicted atmospheric quantities among the set of endmember pixels.



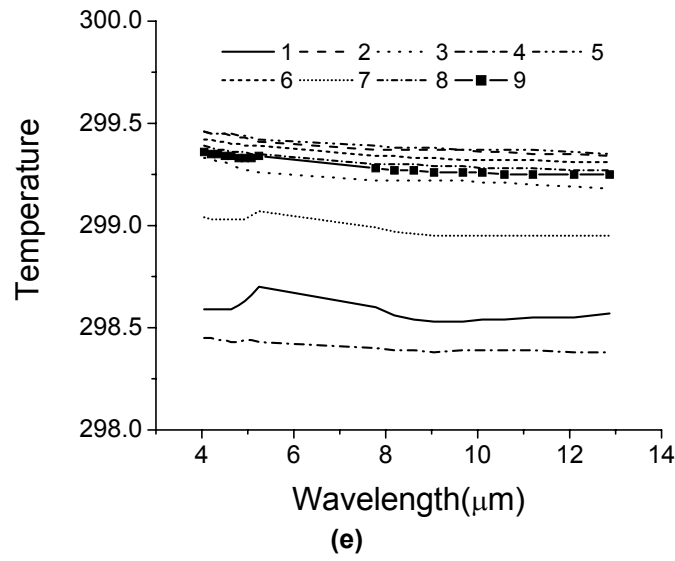
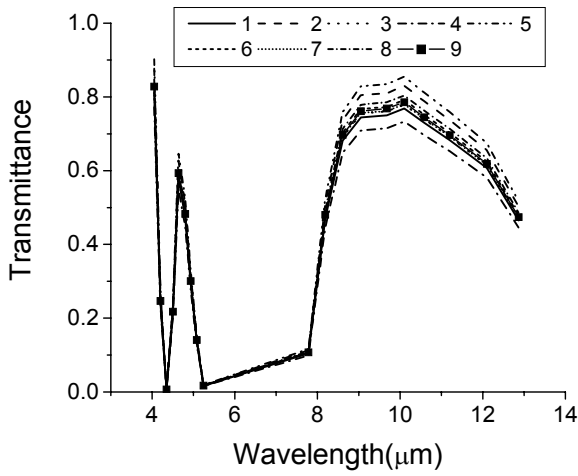
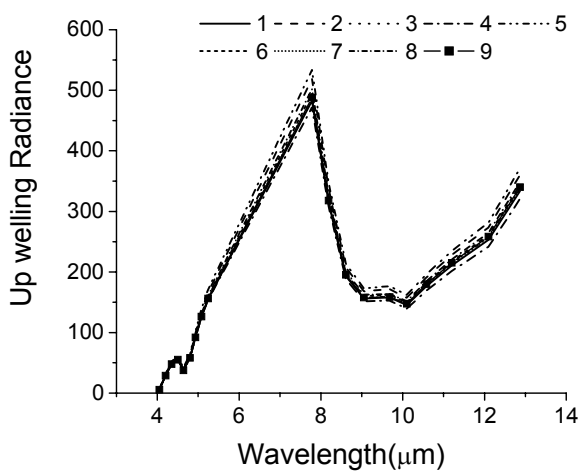


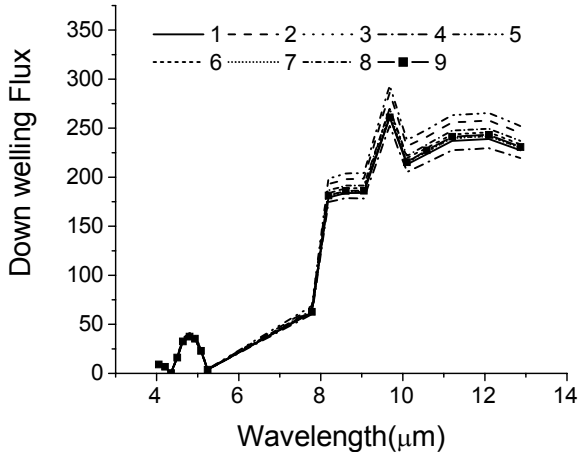
**Figure 5.** Results for atmospheric correction of nine pixel groups using the variable humidity atmospheric basis, (a) transmittance, (b) upwelling radiance (c) downwelling flux, (d) emissivity (e) ground temperature.



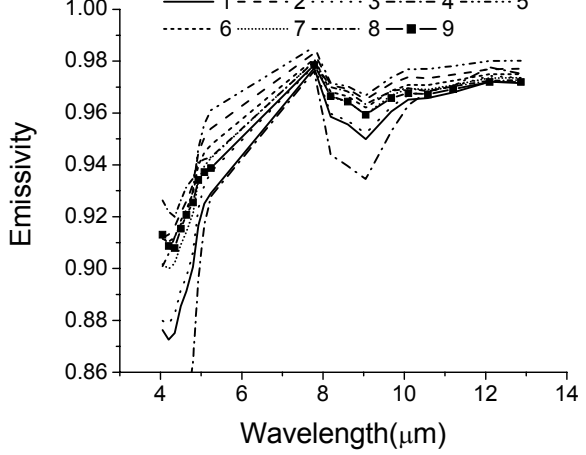
(a)



(b)



(c)



(d)

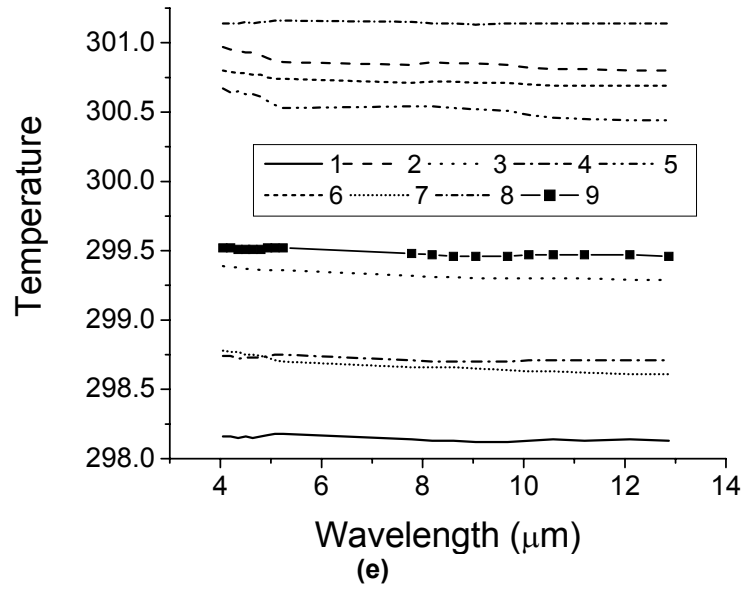


**Figure 6.** Results for atmospheric correction of nine pixel groups using the fixed humidity atmospheric basis, fixed to match the prediction of FLAASH, (a) transmittance, (b) upwelling radiance (c) downwelling flux, (d) emissivity (e) ground temperature.

## CONCLUSIONS

Our approach to TIR atmospheric correction uses a forward model with bases of atmospheric TUDs, emissivities and blackbody emissions. It is a triple expansion with assumptions: (1) the true atmospheric transmittance, upwelling and downwelling radiances are positive linear combinations of the bases of the  $\{t_k, U_k, D_k\}$  derived from MODTRAN, and (2) all quantities related to the ground material(s) are weighted averages of the equivalent basis set quantities. Mathematically, these assumptions are equivalent to assuming that the atmospheric quantities are in the convex cones of the corresponding atmospheric basis quantities and that the ground material quantities are in the convex hull of the derived ground material bases. To derive a pixel temperature, the additional assumption that the pixel contains only one material or the materials in the pixel are at the same temperature is required.

The process of atmospheric correction and emissivity/temperature separation of TIR data is ill-posed. The use of a minimum residual criterion, common to this method and other subspace projection techniques, is hampered by shallow minima, with a variety of combinations of compensating ground and atmospheric conditions leading to close fits to the data. The atmospheric and ground material quantities are strongly coupled and estimating them is sensitive to small variations in emissivity and atmospheric profile. Auxiliary information and constraints make important contributions to reduce the ambiguities. Knowledge about the ground materials allows for smaller, but more relevant emissivity basis sets. The Vis-SWIR data can be used to identify material types and to select pixel groups for TIR atmospheric correction. The variability of the reflectance/emissivity of natural materials in the Vis-SWIR and the TIR spectral regions can be treated through the use of bases of reflectances/emissivities. Additional information about atmospheric conditions can further reduce the parameter space required for the atmosphere description.

The method can be refined by repeating calculations using finer basis grids after initial estimates are made. We are subjecting the method to further testing against synthetic data and we plan to apply it to TIR data for which ground truth is available.

## ACKNOWLEDGEMENTS

This work was supported by the Air Force Research Laboratory/Space Vehicles Directorate under Contract No. F19628-01-C-0016.

## REFERENCES

1. Adler-Golden, S. M., M.W. Matthew, L. S. Bernstein, R. Y. Levine, A. Berk, S. C. Richtsmeier, P. K. Acharya, G. P. Anderson, G. Felde, J. Gardner, M. Hoke, L. S. Jeong, B. Pukall, A. Ratkowski and H.-H Burke, "Atmospheric Correction for Short-wave Spectral Imagery Based on MODTRAN4," *Proc. of SPIE*, **3753** Imaging Spectroscopy V, Denver CO, July 18-23 (1999 ).
2. Gruninger, J, R. L. Sundberg, M. J. Fox, R. Levine, W. F. Mundkowsky, M. S. Salisbury and A. H. Ratcliff, "Automated Optimal Channel Selection for Spectral Imaging Sensors," *Proc. of SPIE*, **4381**, Algorithms for Multispectral and Hyperspectral Imagery VII, Orlando, April 16-19 (2001).
3. Lobell, D.B., G. P. Asner, B.E. Law and R.N. Treuhaft, "Subpixel Canopy Cover Estimation of Coniferous Forests in Oregon using SWIR Imaging Spectrometry," *JGR* **106** D6, 5151-5160 (2001).
4. Asner, G.P., and D.B. Lobell, "A Biogeophysical Approach to Automated SWIR Unmixing of Soils and Vegetation," *Remote Sens. Environ.*, **74**, 99-112, (2000).
5. Bateson, C.A., G.P. Asner, and C.A. Wessman, "End-member Bundles: A New Approach to Incorporating End-member Variability into Spectral Mixture Analysis," *IEEE Transactions on Geosci. and Remote Sensing*, **38**, 1083-1094, (2000).
6. Gruninger, J.H., M.J. Fox and R.L Sundberg, "Hyperspectral Mixture Analysis Using Constrained Projections onto Material Subspaces," *Proceedings International Symposium on Spectral Sensing Research (ISSSR)* Quebec City , June 11-15 (2000).
7. Johnson B. R., S. J. Young, "In Scene Atmospheric Compensation: "Application to SEBASS Data Collected at the ARM Site," Technical Report Aerospace Corporation (1998).
8. Fox , M.J., S.M. Adler-Golden, L.S. Bernstein, G.P. Anderson, and R.D. Kaiser "Atmospheric Correction of MWIR and LWIR Hyperspectral Imagery Using Spectral Smoothness," Technical Report, Spectral Sciences Inc. (2002).
9. Borel, C.C. "Iterative Retrieval of Surface Emissivity and Temperature for a Hyperspectral Sensor" First JPL Workshop on Remote Sensing of Land Surface Emissivity, (1997).
10. Hernandez-Baquero, E.D. and J.R. Schott, "Atmospheric Compensation for Surface Temperature and Emissivity Separation," *Proc of SPIE*, **4049**, Algorithms for Multispectral and Hyperspectral Imagery VI, Orlando, April 24-26 (2000).
11. Villeneuve, P.V., and A. D. Stocker, "Oblique Projection Retrieval of the Atmosphere (OPRA)," *SPIE*, **4725**, Algorithms for Multispectral and Hyperspectral Imagery VII, Orlando, April 1-5 (2002).
12. Healey, G. and D. Slater, "Models and Methods for Automatic Material Identification in Hyperspectral Imagery under Unknown Illumination and Atmospheric Conditions," *IEEE Transactions on Geoscience and Remote Sensing*, **37**, 2706-2717, (1999).
13. Silvey, S. D. "Multicollinearity and Imprecise Estimation," Royal Statistical Soc., Series B, **31**, 539-552, (1969).
14. Lawson, Charles. L, and Hanson, Richard J., "Solving Least Squares Problems," Prentice Hall, Englewood Cliffs, New Jersey, (1974).
15. Hook, S. J., J. J. Myers, K. J. Thome, M. Fitzgerald and A. B. Kahle, " The MODIS/ASTER airborne simulator (MASTER) a new instrument for Earth Science Studies" *Remote Sensing of the Environment*, (2000).
16. ASTER <http://speclib.jpl.nasa.gov>.
17. Wan, Zhengming <http://www.icess.ucsb.edu/~zhang/EMIS/html/em.html>.
18. Collins, E.F., D.A. Roberts, P.C. Sutton, C.C. Funk, and C.C. Borel, "Temperature Estimation and Compositional Mapping Using Spectral Mixture Analysis of Thermal Imaging Spectrometry Data," *Proc. of SPIE*, **3753** , Imaging Spectrometry V, Denver, July 19-21 (1999).